Computationally efficient models of neuromuscular recruitment and mechanics

2008 J. Neural Eng. 5 175

(http://iopscience.iop.org/1741-2552/5/2/008)

J. Neural Eng. **5** (2008) 175–184 doi:10.1088/1741-2560/5/2/008

Computationally efficient models of neuromuscular recruitment and mechanics

D Song[1], G Raphael[1], N Lan[2] and G E Loeb[1]

[1] Department of Biomedical Engineering, University of Southern California, Los Angeles, CA 90089, USA
[2] Division of Biokinesiology and Physical Therapy, University of Southern California, Los Angeles, CA 90089, USA

E-mail: ninglan@usc.edu

Received 23 October 2007
Accepted for publication 20 March 2008
Published 28 April 2008
Online at stacks.iop.org/JNE/5/175

Abstract
We have improved the stability and computational efficiency of a physiologically realistic, virtual muscle (VM 3.∗) model (Cheng *et al* 2000 *J. Neurosci. Methods* **101** 117–30) by a simpler structure of lumped fiber types and a novel recruitment algorithm. In the new version (VM 4.0), the mathematical equations are reformulated into state-space representation and structured into a CMEX S-function in SIMULINK. A continuous recruitment scheme approximates the discrete recruitment of slow and fast motor units under physiological conditions. This makes it possible to predict force output during smooth recruitment and derecruitment without having to simulate explicitly a large number of independently recruited units. We removed the intermediate state variable, effective length (L_{eff}), which had been introduced to model the delayed length dependency of the activation–frequency relationship, but which had little effect and could introduce instability under physiological conditions of use. Both of these changes greatly reduce the number of state variables with little loss of accuracy compared to the original VM. The performance of VM 4.0 was validated by comparison with VM 3.1.5 for both single-muscle force production and a multi-joint task. The improved VM 4.0 model is more suitable for the analysis of neural control of movements and for design of prosthetic systems to restore lost or impaired motor functions. VM 4.0 is available via the internet and includes options to use the original VM model, which remains useful for detailed simulations of single motor unit behavior.

(Some figures in this article are in colour only in the electronic version)

1. Introduction

The original Virtual Muscle™ software (VM 3.∗) (Cheng *et al* 2000) was based on a series of muscle characterization experiments designed specifically to develop an accurate set of mathematical equations representing the physiological processes of force production (Brown *et al* 1999, Brown and Loeb 1999, 2000a, 2000b). The data from those and other experiments were used to fit coefficients to describe the details of recruitment and force generation in skeletal muscles with mixed fiber types. VM 3.∗ includes a motor neuron pool with multiple motor units recruited discretely, in size-ranked order, and with physiological frequency modulation and second-order activation kinetics (Brown and Loeb 2000b). The lumped passive forces and aggregate active forces of all motor units interact with the muscle mass and visco-elastic tendon and aponeurosis (Scott and Loeb 1995). The model differs from the usual Hill-type models in that it includes length dependence of the activation–frequency (Af) and force–velocity (FV) relationships as well as sag and yield behaviors that are fiber-type specific (Brown *et al* 1999, Brown and Loeb 2000b). These processes have usually been ignored or treated independently in other muscle models.

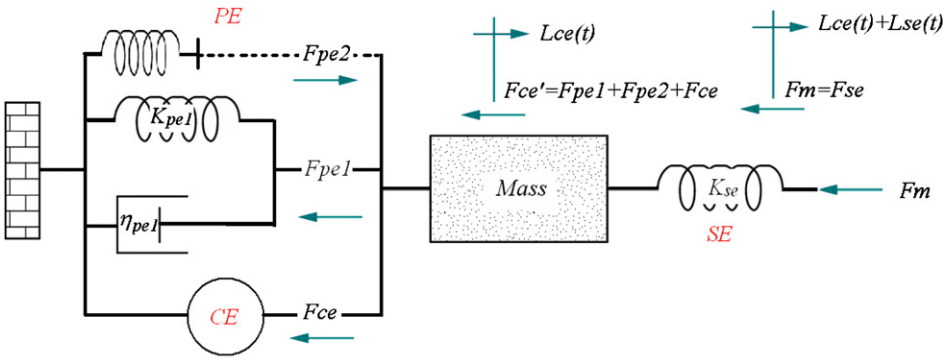

Figure 1. The mechanical structure of a single and lumped unit in the VM model. The contractile element (CE) operates in parallel with the passive element (PE), which consists of stretching (PE1) and compressing components (PE2), to represent the fascicles. The fascicle element is in series with muscle mass element and series-elastic element (SE), which represent the combined tendon and aponeurosis. F_{pe1} results from the well-recognized nonlinear spring K_{pe1} with a viscosity element (η_{pe1}) that resists quick stretch and compression in the passive muscle, while F_{pe2} results from a nonlinear spring K_{pe2} resisting compression at the thick myofilaments during active contraction at short lengths, thus is proportional to the activity of the muscle; F_{se} results from a nonlinear spring K_{se} with a low stiffness toe region. $F_{ce'}$ is the force produced by combined contractile and passive components in the fascicle or contractile element; the difference of $F_{ce'}$ and F_{se} operate on the muscle mass to drive the muscle contraction dynamics.

VM 3.∗ was built in MATLAB with inter-connected Simulink basic blocks, which is inefficient in terms of memory utilization and computational speed. In the new VM, the mathematical equations provided in Cheng *et al* (2000) were re-formulated in state-space representation by explicitly choosing a set of state variables. The state-space model was then implemented in a single CMEX S-function of SIMULINK. The S-function is a computational module of numerical integration, which accepts a set of inputs to the model, updates model states based on their derivative equations, and calculates a set of outputs efficiently. It is represented by a single, customized Simulink block whose inputs and outputs can be linked to other Simulink blocks representing the other parts of the mechanical and control system. Such model implementation is convenient for neurophysiologists to build their own models efficiently using VM blocks for each muscle.

VM 3.∗ was intended as a generic modeling tool for public use in neuromuscular physiology and engineering applications. In this study, we evaluated its computational performance in realistic multi-muscle and multi-joint settings. These simulations revealed that smooth modulation of force output could only be obtained with a large number of discrete motor units, which resulted in excessively long computational time. There was also an instability in the interaction of antagonistic muscles around a joint that was traced to the intermediate state variable, effective length (L_{eff}), which had been introduced to model the delayed length dependence of the activation–frequency relationship. These problems were fixed in VM 4.0 and validated against VM 3.1.5 as presented here.

A new muscle recruitment algorithm called 'natural continuous' approximates the discrete recruitment of individual units in the original VM 3.∗. The new recruitment strategy lumps multiple motor units of the same muscle fiber type into a single motor unit that is frequency modulated (see below). This greatly reduces the number of motor units needed to generate a smooth recruitment response. The new natural continuous recruitment algorithm weights the force output of the lumped motor units within a fiber type and between the fiber types to give rise to smooth force production over the entire range of activation levels. Preliminary results have been presented elsewhere (Song *et al* 2007).

VM 4.0 includes both the old and the new recruitment schemes, making it suitable for analysis of neural control of movements (Alstermark *et al* 2007, Chan and Moran 2006, Lan *et al* 2005), and for design of prosthetics and FES systems to restore lost or impaired motor functions. VM 4.0 is available for downloading from http://ami.usc.edu/projects/ami/projects/bion/musculoskeletal/virtual_muscle.html.

2. Material and methods

2.1. Musculotendon dynamics

The musculotendon dynamics of the VM model is modeled as a second-order mechanical system which includes the muscle mass driven by the difference of forces generated in contractile element (fascicle) and series element (tendon) (figure 1).

2.2. Recruitment types

VM 4.0 allows the user to build four different models of a given muscle based on the recruitment strategy:

- Natural discrete (Brown and Cheng) provides the original VM 3.∗ model with discrete motor units and effective length (L_{eff}) and produces an output consisting of nested Simulink blocks.
- Natural discrete provides the VM 4.0 model (L_{eff} omitted; single S-function output) with discrete motor units and size-ordered recruitment similar to VM 3.∗.
- Natural continuous provides the VM 4.0 model with a single motor unit of each fiber type that is frequency modulated and weighted to approximate size-ordered physiological recruitment.

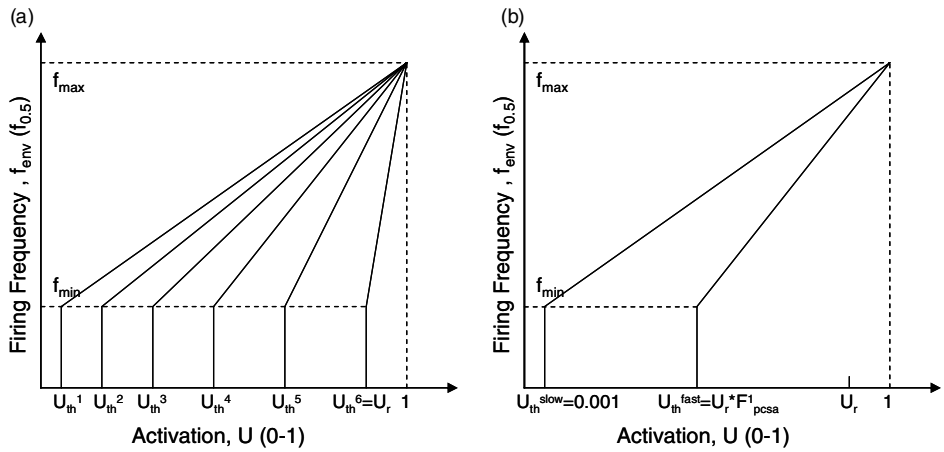

Figure 2. (a) Natural discrete recruitment algorithm as applied to a muscle consisting of three simulated slow-twitch and three fast-twitch motor units, respectively. U_{th}^i is the recruitment threshold of ith motor unit; U_r is the activation level at which all the motor units are recruited. Once a motor unit is recruited, the firing frequency of the unit will rise linearly with U between $f_{\min}$ and $f_{\max}$. This recruitment scheme mimics biologic recruitment of motor neurons. (b) Natural continuous recruitment algorithm as applied to two fiber types, slow and fast. U_{th}^i is the recruitment threshold of ith fiber type or unit; the first fiber type $U_{\text{th}}^1 = U_{\text{th}}^{\text{slow}}$ is fixed at 0.001. Similar to the discrete algorithm, once a fiber type is recruited, the firing frequency of the fiber will rise linearly with U between $f_{\min}$ and $f_{\max}$.

- Intramuscular FES provides the VM 4.0 model with a single motor unit of each fiber type whose frequency of firing is specified by an input variable representing stimulus frequency. Force output is weighted equally among the motor units to approximate the random fiber-type recruitment reported for intramuscular electrical stimulation by Singh *et al* (2000).

One important feature of the virtual muscle model is the built-in recruitment scheme of multiple motor units for different fiber types. The natural discrete algorithm in VM 3.∗ was formulated to model the multiple motor neuron pool and natural orderly recruitment of motor units (figure 2(a)) in response to the neural activation input, U (Cheng *et al* 2000). Activation incrementally recruits the motor units based on the recruitment rank of the fiber type, and once the unit is recruited, the firing frequency input of this unit (f_{env}) start from a nonzero value (from $f_{\min} = 0.5\ f_{0.5}$ to $f_{\max} = 2\ f_{0.5}$) and is modulated linearly over a range of frequencies specific to the unit type. The default range is a function of $f_{0.5}$, the frequency for which the steadily recruited motor unit produces 50% of its maximal tetanic force, F_0, at its optimal fascicle length, L_{ce0}. This neural excitation signal is modeled as two separate first-order dynamics (f_{env}–f_{int}–f_{eff}) to simulate the rise and fall time of calcium kinetics (Brown and Loeb 2000b). The level of effective activation of each fiber type results from a linear combination of multiple motor unit activations (Af) weighted by their respective fractional PCSA (physiological cross-sectional area). The differences between slow and fast fiber types are reflected in rise–fall times of excitation dynamics, sagging (S) or yielding (Y) properties, Af relation and muscle force–length, force–velocity (FL, FV) properties. The sudden recruitment of a motor unit at its initial firing rate causes a step increase of muscle force; the size of that step is determined by the fractional PCSA of that unit, which is a function of the number of motor units modeled in the pool. If the number of motor units is sufficiently large (e.g. ∼100 as occurs in a typical muscle), the factional PCSA can be reduced to produce a relatively smooth recruitment of muscle force. In order to reduce computational time, however, VM models are often constructed with only a few motor units, so the step jump in force recruitment is unphysiologically large, particularly at low levels of activation.

To solve this problem, we designed a natural continuous algorithm (figure 2(b)) to match the average behavior of the natural discrete recruitment strategy. Instead of modeling each unit explicitly, the natural continuous algorithm lumps the multiple units according to the corresponding fiber types, thus requiring only one unit per fiber type. Each unit or fiber type becomes active at a threshold U_{th}^i that depends on the distribution of fractional PCSA (F_{pcsa}) among all the fiber types and their recruitment orders

$$\begin{cases} U_{\text{th}}^i = 0.001 & i = 1 \\ U_{\text{th}}^i = U_r \cdot \sum_{k=1}^{i-1} F_{\text{pcsa}}^k & i > 1. \end{cases} \tag{1}$$

Once recruited, the lumped motor unit modulates its frequency according to the usual calcium dynamics as in the natural discrete algorithm. There are three important aspects of the new algorithm. First, the total muscle activation and contraction dynamics depend on the proportions of slow and fast fibers. The continuous algorithm accounts for this effect by linearly combining Af and FL, the FV properties of each fiber types (equation (2)) multiplied by a weighting factor, W^i, representing proportions of the fiber type among the overall active muscle portion (equation (3)). Second, the discrete algorithm simulates force modulations in physiological muscles by sequentially adding or subtracting fractional PCSA-scaled forces of newly recruited or derecruited motor units. As the number of units increases, this additional

process is equivalent to multiplication by the activation level (U_{eff}), which formulates the continuous version of neural modulation of muscle forces in the new natural continuous algorithm (equation (2)). Third, the activation–frequency (Af) relationship includes the dynamics of calcium activation and this effect must also be represented in the multiplication of activation. We thus introduced a first-order dynamics to convert activation input U to effective activation U_{eff} (equation (4)). The values of rising and falling time constants (T_U) were chosen to simulate the dynamic force responses of natural discrete system to sinusoidal activation inputs over the range of physiological neural modulations (0–10 Hz).

The normalized active force from contractile element (CE) with n fiber types (units) is calculated as

$$\bar{F}_{\text{ce}} = U_{\text{eff}} \cdot \sum_{i=1}^{n} [W^i \cdot \text{Af}^i \cdot (\text{FL}^i\text{FV}^i + \bar{F}_{\text{pe2}})], \tag{2}$$

where n is the number of active muscle fiber types and W^i is calculated based on the threshold of each fiber type or unit, U^i_{th}, and the effective activation, U_{eff},

$$W^i = \frac{U_{\text{eff}} - U^i_{\text{th}}}{\sum_{k=1}^{i} \left(U_{\text{eff}} - U^k_{\text{th}}\right)}, \qquad \forall\, U_{\text{eff}} \geqslant U^i_{\text{th}}. \tag{3}$$

The amount of muscle actually recruited is specified by an intermediate muscle activation signal, effective activation, U_{eff}, which incorporates first-order dynamics simulating the rise–fall effect modeled in calcium dynamics

$$\dot{U}_{\text{eff}} = \frac{U - U_{\text{eff}}}{T_U}, \qquad T_U = \begin{cases} 0.03(\text{sec}) & U \geqslant U_{\text{eff}} \\ 0.15(\text{sec}) & U < U_{\text{eff}}. \end{cases} \tag{4}$$

2.3. Contractile dynamics

A realistic model of the human elbow and shoulder was constructed from six VM 3.∗ muscles as described in (Song *et al* at press). As described under the results of section 3.1., this model exhibited unphysiological instability that was traced to the intermediate state variable, effective length (L_{eff}), which was modeled in VM 3.∗ using a nonlinear first-order differential equation

$$\dot{\bar{L}}^{\text{eff}\,i}_{\text{ce}}(t) = \frac{\left[\bar{L}_{\text{ce}}(t) - \bar{L}^{\text{eff}\,i}_{\text{ce}}(t)\right]^3}{T_L(1 - \text{Af}^i)} \tag{5}$$

(L_{eff} described in the text and figures is an abbreviation of 'effective length' and it is represented by $\bar{L}^{\text{eff}}_{\text{ce}}$ in equations, which denotes the normalized effective length of muscle contractile element).

The construct of effective length (L_{eff}) was introduced in VM 3.∗ to model the delayed length dependence of the activation–frequency (Af) relationship (Brown *et al* 1999). The activation process that determines which cross-bridges can contribute active force acts with a delay, so any mechanical effects of length on the activation process itself will be related to the length of the muscle at that earlier time, rather than the current length and velocity, which exert their effects on the cross-bridges themselves (Brown *et al* 1999). This is a relatively subtle effect that can be revealed by appropriate experimental design under conditions of controlled activation and kinematics (Brown *et al* 1999). To model this effect, (Cheng *et al* 2000) replaced the length input to the Af relationship with a time-delayed version of length (effective length: L_{eff}) as seen in equation (6)

$$Af^i = \begin{cases} \text{Af}^i\left(f^i_{\text{eff}}, \bar{L}^{\text{eff}^i}_{\text{ce}}, \bar{V}_{\text{ce}}\right) = 1 - \exp\left[-\left(\dfrac{Yf^i_{\text{eff}}}{a_f n_f}\right)^{n^i_f}\right], \\ \qquad\qquad \text{slow} \\ \text{Af}^i\left(f^i_{\text{eff}}, \bar{L}^{\text{eff}^i}_{\text{ce}}\right) = 1 - \exp\left[-\left(\dfrac{S^i f^i_{\text{eff}}}{a_f n_f}\right)^{n^i_f}\right], \\ \qquad\qquad \text{fast} \end{cases}$$
$$n^i_f = n_{f0} + n_{f1}\left(\frac{1}{\bar{L}^{\text{eff}^i}_{\text{ce}}} - 1\right) \tag{6}$$

The destabilizing effect is removed by omitting L_{eff}, and the new Af relationship is then modeled as a function of current muscle fascicle length (equation (7)). The performances of these two versions of the muscle model are compared in the results of section 3.1,

$$\text{Af}^i = \begin{cases} \text{Af}^i\left(f^i_{\text{eff}}, \bar{L}_{\text{ce}}, \bar{V}_{\text{ce}}\right) = 1 - \exp\left[-\left(\dfrac{Yf^i_{\text{eff}}}{a_f n_f}\right)^{n^i_f}\right], \\ \qquad\qquad \text{slow} \\ \text{Af}^i\left(f^i_{\text{eff}}, \bar{L}_{\text{ce}}\right) = 1 - \exp\left[-\left(\dfrac{S^i f^i_{\text{eff}}}{a_f n_f}\right)^{n^i_f}\right], \\ \qquad\qquad \text{fast} \end{cases}$$
$$n^i_f = n_{f0} + n_{f1}\left(\frac{1}{\bar{L}_{\text{ce}}} - 1\right) \tag{7}$$

Table 1 provides the complete equations and coefficients for human muscle fiber types in the reformulated virtual muscle model.

2.4. Validation

To test the effectiveness of the natural continuous strategy, we compared its performance with that of the natural discrete VM model for both static and dynamic conditions of activation and kinematics. A human muscle model (deltoid posterior) with motor neuron pool composed of 60% slow and 40% fast fiber types was used. The muscle mass was 97.5 g (i.e. $F_0 = 266$ N), optimal fascicle length was 11 cm, optimal tendon length was 2 cm and maximal musculotendon length was 18.4 cm. Static force–activation relationships (F–U curves) of natural discrete muscle models with a small number of motor units (three slow and three fast) and with a more physiological motor pool (30 slow and 30 fast) were compared with those of the natural continuous muscle model at constant muscle length input ($L_{\text{mt}} = 16$ cm) over the full range of activation levels ($U =$ 0–1).

The natural discrete algorithm models multiple units which differ in the distributions of firing rates that they produce

Table 1. Summary of model equations and best-fit constants.

Equations	Slow-twitch fibers				Fast-twitch fibers			
$\bar{F}_{se}(\bar{L}_{se}) = c^T k^T \ln\left\{\exp\left[\frac{\bar{L}_{se}-L_r^T}{k^T}\right]+1\right\}$	c^T	k^T	L_r^T		c^T	k^T	L_r^T	
	27.8	.0047	0.964		27.8	.0047	0.964	
$\bar{F}_{pe1}\left(\bar{L}_{ce}, \bar{V}_{ce}\right) = c_1 k_1 \ln\left\{\exp\left[\frac{\bar{L}_{ce}/\bar{L}_{ce}^{max}-L_{r1}}{k_1}\right]+1\right\}+\eta\bar{V}_{ce}$	c_1	k_1	L_{r1}	η	c_1	k_1	L_{r1}	
	23.0	0.046	1.17	0.01	23.0	0.046	1.17	
$\bar{F}_{pe2}\left(\bar{L}_{ce}\right) = c_2\left\{\exp\left[k_2\left(\bar{L}_{ce}-L_{r2}\right)\right]-1\right\},\ \bar{F}_{pe2}\leqslant 0$	c_2	k_2	L_{r2}		c_2	k_2	L_{r2}	
	−0.02	−21.0	0.70		−0.02	−21.0	0.70	
$FL\left(\bar{L}_{ce}\right) = \exp\left(-\left\lvert\frac{\bar{L}_{ce}^{\beta}-1}{\omega}\right\rvert^{\rho}\right)$	ω	β	ρ		ω	β	ρ	
	1.12	2.30	1.62		0.75	1.55	2.12	
$FV\left(\bar{V}_{ce}, \bar{L}_{ce}\right) =$ $\begin{cases}\left(V_{max}-\bar{V}_{ce}\right)/\left[V_{max}+\left(c_{v0}+c_{v1}\bar{L}_{ce}\right)\bar{V}_{ce}\right], & \bar{V}_{ce}\leqslant 0\\ \left[b_v-\left(a_{v0}+a_{v1}\bar{L}_{ce}+a_{v2}\bar{L}_{ce}^2\right)\bar{V}_{ce}\right]/\left(b_v+\bar{V}_{ce}\right), & \bar{V}_{ce}>0\end{cases}$	V_{max}	c_{v0}	c_{v1}		V_{max}	c_{v0}	c_{v1}	
	−7.88	5.88	0		−9.15	−5.70	9.18	
	a_{v0}	a_{v1}	a_{v2}	b_v	a_{v0}	a_{v1}	a_{v2}	b_v
	−4.70	8.41	−5.34	0.35	−1.53	0	0	0.69
$\begin{cases}\mathrm{Af}^i\left(f_{eff}^i, \bar{L}_{ce}, \bar{V}_{ce}\right) = 1-\exp\left[-\left(\frac{Yf_{eff}^i}{a_f n_f}\right)^{n_f^i}\right], & \text{slow}\\ \mathrm{Af}^i\left(f_{eff}^i, \bar{L}_{ce}\right) = 1-\exp\left[-\left(\frac{S^i f_{eff}^i}{a_f n_f}\right)^{n_f^i}\right], & \text{fast}\end{cases}$ $n_f^i = n_{f0}+n_{f1}\left(\frac{1}{L_{ce}}-1\right)$	a_f	n_{f0}	n_{f1}		a_f	n_{f0}	n_{f1}	
	0.56	2.1	5		0.56	2.1	3.3	
$\dot{Y}(t) = \frac{1-c_Y\left[1-\exp\left(-\frac{\lvert\bar{V}_{ce}\rvert}{V_Y}\right)\right]-Y(t)}{T_Y}$	c_Y	V_Y	$T_Y(ms)$		–	–	–	
	0.35	0.1	200					
$\dot{S}^i\left(t, f_{eff}^i\right) = \frac{a_S-S^i(t)}{T_S},\ a_S = \begin{cases}a_{S1}, & f_{eff}^i(t)<0.1\\ a_{S2}, & f_{eff}^i(t)\geqslant 0.1\end{cases}$	–	–	–		a_{S1}	a_{S2}	$T_S(ms)$	
					1.76	0.96	43	
$\dot{f}_{int}^i\left(t, f_{env}^i, \bar{L}_{ce}\right) = \frac{f_{env}^i(t)-f_{int}^i(t)}{T_f^i}$ $\dot{f}_{eff}^i\left(t, f_{int}^i, \bar{L}_{ce}\right) = \frac{f_{int}^i(t)-f_{eff}^i(t)}{T_f^i}$ $T_f^i = \begin{cases}T_{f1}\bar{L}_{ce}^2+T_{f2}f_{env}^i(t), & \dot{f}_{eff}^i\geqslant 0\\ \left(T_{f3}+T_{f4}Af^i\right)/\bar{L}_{ce}, & \dot{f}_{eff}^i<0\end{cases}$	$T_{f1}(ms)$	$T_{f2}(ms)$	$T_{f3}(ms)$	$T_{f4}(ms)$	$T_{f1}(ms)$	$T_{f2}(ms)$	$T_{f3}(ms)$	$T_{f4}(ms)$
	34.3	22.7	47.0	25.2	20.6	13.6	28.2	15.1
$\dot{U}_{eff} = \frac{U-U_{eff}}{T_U},\ T_U = \begin{cases}T_{U1} & U\geqslant U_{eff}\\ T_{U2} & U<U_{eff}\end{cases}$	$T_{U1}(ms)$	$T_{U2}(ms)$			$T_{U1}(ms)$	$T_{U2}(ms)$		
	30	150			30	150		

Notes. Top bar $\bar{x}$ denotes the normalized variable x (forces by maximum isometric tetanic muscle force F_0, lengths and velocities by optimal fascicle length or optimal tendon length [L_{ce0} or L_{se0}]); superscript x^i denotes the ith motor unit specific variable x.

Table 2. Symbols and the definitions.

Symbols	Definitions
U	Activation input (0–1)
F^i_{pcsa}	Fractional PCSA of ith motor unit (0–1)
U^i_{th}	Recruitment threshold for ith motor unit (0–1)
U_r	Fractional activation level at which all motor units for a given muscle are recruited (0–1)
U_{eff}	Effective activation, an intermediate muscle activation signal simulating calcium dynamics (0–1)
W^i	Proportion of active ith fiber-type/motor unit of total active muscle (0–1)
F_0	Muscle maximal tetanic force (N)
L_{ce0}	Optimal fascicle length (cm)
L_{se0}	Optimal tendon length (cm)
$\bar{F}_{\text{se}}$	Series elastic element (tendon) force (F_0)
$\bar{F}_{\text{pe1}}$	Stretching contractile passive element (fascicle) force (F_0)
$\bar{F}_{\text{pe2}}$	Compressive contractile passive element (fascicle) force (F_0)
$\bar{F}_{\text{ce}}$	Active contractile element force (F_0)
$\bar{F}_{\text{ce}'}$	Total contractile element force (F_0)
$\bar{L}_{\text{se}}$	Tendon length (L_{se0})
$\bar{L}_{\text{ce}}$	Fascicle length (L_{ce0})
$\bar{L}^{\max}_{\text{ce}}$	Maximum fascicle length of the muscle at its maximum anatomic musculotendon length (L_{ce0})
$\bar{V}_{\text{ce}}$	Fascicle velocity (L_{ce0}/s)
FL^i	Force-length function of ith muscle fiber type
FV^i	Force–velocity function of ith muscle fiber type
Af^i	Activation–frequency relationship of ith motor unit
Y	Yielding factor for slow motor units
S^i	Sagging factor for ith fast motor unit
f^i_{env}	Firing frequency input to second-order excitation dynamics of ith motor unit ($f_{0.5}$)
f^i_{int}	Intermediate firing frequency of second-order excitation dynamics of ith motor unit ($f_{0.5}$)
f^i_{eff}	Effective firing frequency of ith motor unit ($f_{0.5}$)
$\bar{L}^{\text{eff}\,i}_{\text{ce}}$	Effective fascicle length (L_{ce0})

in the various muscle fibers at different levels of activation. Frequency of firing has complex effects on the dynamics of the contractile apparatus and its FL, FV properties that are also fiber-type specific. Therefore, we compared the predicted force for the natural discrete model with 30 units of each type to the natural continuous model during sinusoidal modulation of activation ($U = 0$–1) at constant muscle length ($L_{\text{mt}} = 16$ cm) and during sinusoidal length input from anatomical minimum to maximum ($L_{\text{mt}} = 14$–18 cm corresponding to the range of joint motion) at constant activation level ($U = 0.5$). Because the activation dynamics include delay terms, we systematically varied the frequency of sinusoidal modulation of activation (U) over the range 1–10 Hz.

3. Results

3.1. Stability

VM 3.∗ ('natural discrete (Brown and Cheng)' in VM 4.0) introduced an intermediate state variable, effective length (L_{eff}), to model the effect of delayed length dependence on activation–frequency relationships (Af) (equation (6)). This forms an internal negative feedback loop between muscle activation and musculotendon length with an Af-dependent delay, which may produce instability of the musculoskeletal dynamics even without reflex feedback (figure 3(a)). Removing this variable (equation (7)) resulted in a stable open-loop response as shown in figure 3(b). Computation time was also significantly reduced after removing the state variable of effective length (see figure 7).

3.2. Accuracy for static conditions

The natural continuous and natural discrete recruitment schemes were compared first in isometric contraction of the deltoid posterior muscle models at constant muscle length, 16 cm. The F–U curves of discrete model with 3 units and 30 units for each fiber type were superimposed with that of continuous muscle in figure 4. The continuous recruitment strategy demonstrated a similar profile of F–U relationship over the full range of activation ($U = 0$–1 in figure 4(a)). However, for the discrete model with fewer motor units (three slow and three fast) the finer scale of the curve ($U = 0$–0.3) revealed abrupt jumps in force (∼15N) associated with stepwise recruitment of the slow units (figure 4(b)). This effect was mitigated as the number of units increases. As expected, the natural continuous recruitment strategy provided essentially a smoothed version of the same output forces, closer to what would be expected for a real muscle consisting of a much larger number of discrete motor units.

3.3. Accuracy for dynamic conditions

To test the effectiveness of the natural continuous algorithm in modeling the dynamic response of muscle to neural modulation and muscle length changes, the force outputs of the continuous muscle model were compared with those of the natural discrete model under input conditions of sinusoidal U at constant L_{mt} (figure 5(a)); and a sinusoidal L_{mt} at constant U (figure 5(b)). The continuous model produced force transients approximating those of the discrete model in response to both

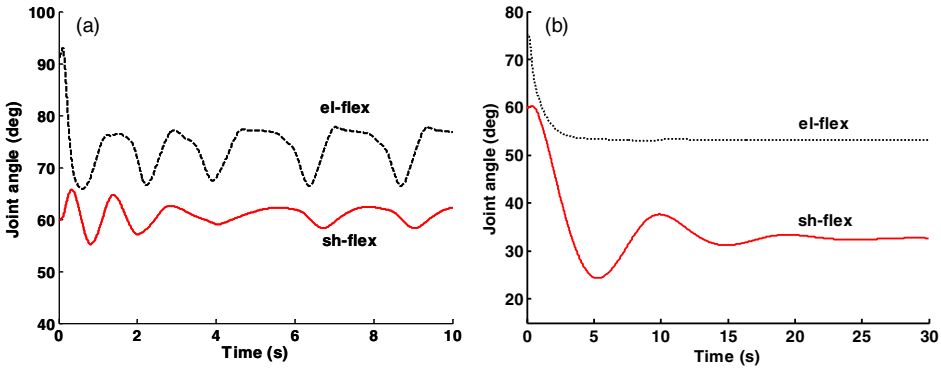

Figure 3. Simulations in (a) and (b) are actuated by discretely recruited muscle models with and without L_{eff}. (a) A demonstration of the instability caused by L_{eff} in virtual muscle through an open-loop dynamic simulation using a 2-DOF-6-muscle arm model. The muscle activation commands of the antagonist muscles across shoulder (sh), elbow (el) and both joints (bi): $U_{\text{sh}} = 0.9$, $U_{\text{el}} = 0.4$, $O_{\text{bi}} = 0.0$. (b) A demonstration of stable open-loop response at the shoulder and elbow joints after removal of the effective length state.

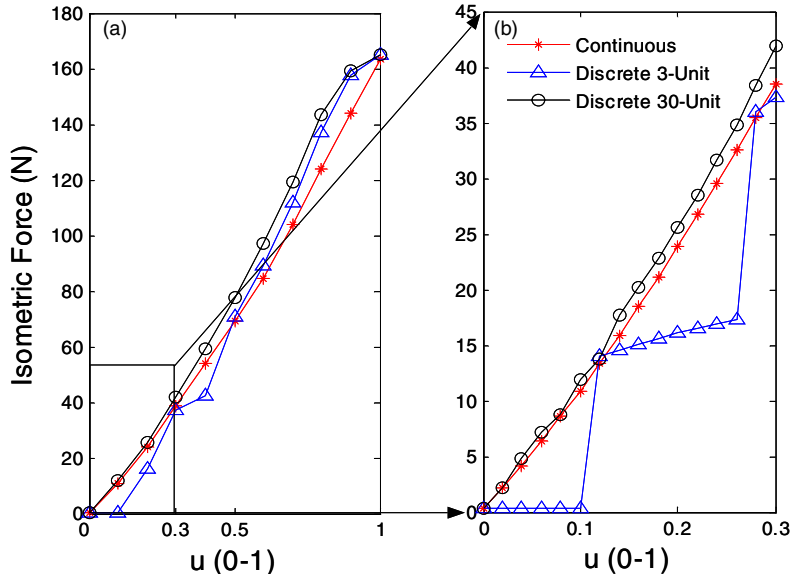

Figure 4. The comparison of steady-state force-activation (F–U) profiles of deltoid posterior at $L_{\text{mt}} = 16$ cm between the natural continuous algorithm and natural discrete models with a small motor neuron pool (three slow and three fast motor units) and a large motor neuron pool (30 slow and 30 fast motor units). All the models have 60% slow fibers and 40% fast fibers. (a) F–U curves spanning entire activation rage ($U = 0$–1); (b) F–U curves zoomed in at the low activation levels ($U = 0$–0.3).

dynamic muscle activation and muscle length changes. There was a slight phase lead for the continuous recruitment strategy during relatively rapid modulation of neural activation U (figure 5(c)). In neural modulation of movement dynamics, the important control variables of muscle output usually include the mean force and force modulation ranges (top panel of figure 5(e)). The ratios of continuous-to-discrete recruitments for these two variables were close to unity over the physiological range of modulation of activation U (1–10 Hz) (figure 5(e)).

The effect of removing L_{eff} on model accuracy was assessed by comparing the same set of sinusoidal modulations of activation and length in the two versions of the model (equation (6) versus (7)). Figure 6 illustrated that the discrepancy of force production between the muscle models with and without effective length is less than 1%.

3.4. Simulation speed

The time elapsed to compute force output for models with different recruitment strategies and different model implementations were compared in figure 7. In the comparison, two second simulations with a single muscle were carried out in Matlab 7.1/Simulink 6.3 on a HP workstation (3.2 GHz Intel® Pentium® 4CPU, 2.0 GB of RAM). In the two discrete models, the computation time increased linearly with number of motor units. Removing the effective length substantially reduced the CPU time. The natural continuous model achieved a 15-fold reduction of computation time

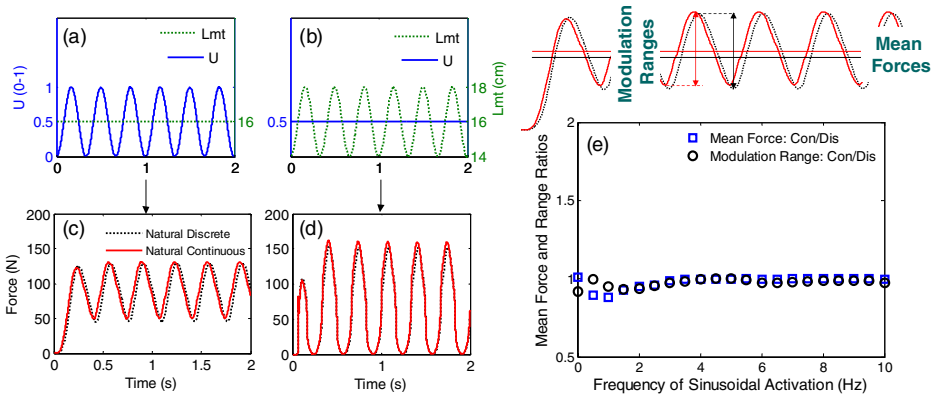

Figure 5. Comparison of dynamic responses between the natural continuous muscle model and natural discrete muscle model with large motor neuron pool (30 slow and 30 fast motor units). Both models have 60% slow fibers and 40% fast fibers. (c) shows the dynamic force responses given the muscle inputs depicted in (a), sinusoidal activation (U: 0–1 at 3 Hz) and constant length ($L_{mt} = 16$ cm); (d) shows the dynamic force responses given the muscle inputs depicted in (b), sinusoidal muscle length (L_{mt}: 14–18 at 3 Hz) and constant activation ($U = 0.5$). (e) shows the ratios of mean forces and force modulation ranges between the continuous and discrete models over the physiological range of modulation of activation U (1–10 Hz).

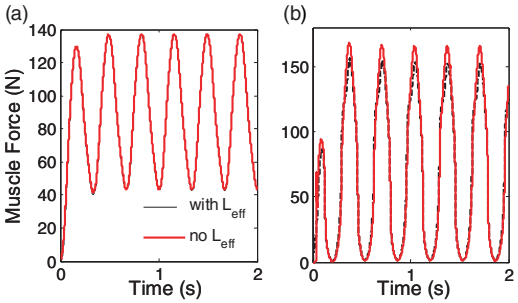

Figure 6. Comparison of dynamic force responses between the natural discrete muscle models with and without effective lengths (L_{eff}). The models include a large motor neuron pool (30 slow and 30 fast motor units). Both models have 60% slow fibers and 40% fast fibers. (a) shows the dynamic force responses to the sinusoidal activation (U: 0–1 at 3 Hz) and constant length ($L_{mt} = 16$ cm) inputs; (b) shows the dynamic force responses to sinusoidal muscle stretching (L_{mt}: 14–18 at 3 Hz) and constant activation ($U = 0.5$) inputs.

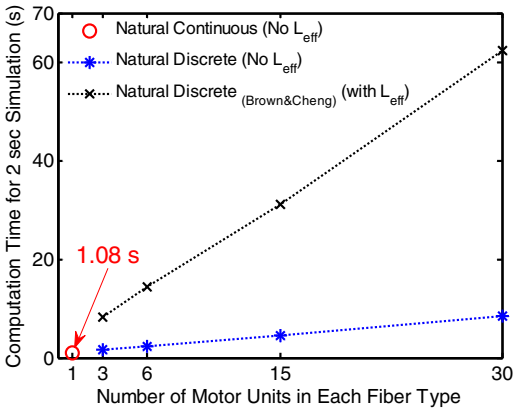

Figure 7. The comparison of computation time of different recruitment models and implementation. The original natural discrete model by Brown and Cheng includes L_{eff} and is implemented by interconnected Simulink basic blocks; the natural discrete and natural continuous models do not include L_{eff} and are implemented using Simulink CMEX S-functions.

compared to the discrete model with 30 motor units and without L_{eff}.

4. Discussion

Muscles are organized into motor units, each consisting of a motor neuron plus a homogeneous group of muscle fibers that are activated synchronously by that motor neuron. Motor units are generally recruited in an orderly sequence based on both the fiber type and the size (PCSA) of the unit (Cheng *et al* 2000). The original VM model (natural discrete) was conceived to simulate this behavior of individual motor unit recruitment in response to a common synaptic excitation to all of the motor neurons in the pool. This is an important feature not present in the most other muscle models and is useful for modeling details of intramuscular mechanics such as the responses of Golgi tendon organs (Mileusnic and Loeb 2006). Ideally, for the natural discrete recruitment to be realistic, the number of motor units included in the model should approach the actual number of motor units in the muscle being modeled, which is often more than 100. Each motor unit adds three states to the model (after removing L_{eff}), substantially increasing the computational time (figure 7).

The natural continuous recruitment scheme introduced in VM 4.0 improves the computational efficiency of the model without significant loss of its physiological realism and accuracy. Lumping motor units into one single structure has been done successfully in another influential muscle model (Zajac 1989), but the physiologically and mechanically different fiber types were not represented at all. The results of static force generation show that the continuous strategy approximates the natural recruitment behavior of motor units very well in the full range of motor neuron pool recruitment

(figure 4). Dynamic simulation also shows that the natural continuous strategy is accurate for the dynamics of force output while requiring only one unit for each fiber type in the muscle (figure 5). The slight discrepancy in force output dynamics (figures 5(c) and (e)) arises because the continuous algorithm replaces the distribution of firing frequencies across individual motor units with a single frequency of the same fiber type that is modulated smoothly according to activation.

Recently, there has been considerable interest in the variability of force output actually produced by muscles under steady-state conditions of kinematics and activation, i.e. motor noise. The amplitude of the noise tends to be a constant fraction of the mean force being generated, i.e. signal-dependent noise or constant coefficient of variance. This has been attributed to the incremental recruitment and derecruitment of motor units whose size is related to their recruitment order (Jones *et al* 2002). Minimizing motor variability has been proposed as an organizational principle for movement control (Hamilton and Wolpert 2002, Harris and Wolpert 1998). In a simulation study to investigate how muscle stiffness may be controlled to minimize kinematic variability in the presence of motor noise (Selen *et al* 2005), the authors proved that the lumped Hill-type muscle model with a single motor unit cannot replicate the realistic force variability. Instead, a motor neuron pool model with 60 motor units combined with Hill-type muscle dynamics must be used. In the VM model, the natural discrete recruitment algorithm is appropriate to replicate the signal-dependent feature of motor noise if the range of sizes of motor units is constructed appropriately and the activation signal has constant noise added to simulate membrane noise. Alternatively, the natural continuous model can be used with signal-dependant activation noise on its input, but the actual amplitude of the output force noise will depend on the low-pass filtering properties of the contractile apparatus.

VM 4.0 also includes a model of recruitment by electrical stimulation (Intramuscular FES) that is designed to simulate the recruitment produced during functional electrical stimulation using intramuscular electrodes (Singh *et al* 2000). As the stimulation pulse strength (equivalent to the activation input) is increased, motor units tend to be recruited at random because threshold depends mostly on distance of the motor axon from the electrode, which is unrelated to unit type or size. Motor units that are activated fire one and only one action potential for each stimulation pulse. Electrodes placed on the muscle nerve or on the surface of skin may produce different patterns of motor unit recruitment. A general recruitment scheme for FES could not be formulated to account for all stimulation techniques. A discrete model similar to the natural discrete recruitment scheme could be constructed if sufficient characterization information were available regarding the expected recruitment order of the individual motor units.

5. Conclusion

The second generation of virtual muscle software (VM 4.0) described in this paper substantially reduces the computational load, and improves the robustness and stability of force computation, particularly when modeling multiple muscles connected to a skeletal linkage. The discrete model of recruitment (natural discrete) is useful to study the detailed effects of the recruitment of individual motor units, such as motor noise (Jones *et al* 2002). The lumped model with the new natural continuous scheme is much more efficient for computation with little loss of accuracy. The ability to easily modify and accurately represent various types of fibers in mixed and/or pathological muscles should be useful for applications of the VM software to neurophysiology, rehabilitation (FES) and sports medicine.

Acknowledgments

This material is based upon work supported by the National Science Foundation under grant IOB 0352117, and Alfred E Mann Institute for Biomedical Engineering at the University of Southern California. The authors would like to thank Dr Rahman Davoodi and Mr Mehdi Khachani for their technical support of Virtual Muscle 4.0 software testing and release.

References

Alstermark B, Lan N and Pettersson L-G 2007 Building a realistic neuronal model that simulates multi-joint arm and hand movements in 3D-space *HFSP J.* **1** 209–14

Brown I E, Cheng E J and Loeb G E 1999 Measured and modeled properties of mammalian skeletal muscle: II. The effects of stimulus frequency on force-length and force–velocity relationships *J. Muscle Res. Cell Motil.* **20** 627–43

Brown I E and Loeb G E 1999 Measured and modeled properties of mammalian skeletal muscle: I. The effects of post-activation potentiation on the time course and velocity dependencies of force production *J. Muscle Res. Cell Motil.* **20** 443–56

Brown I E and Loeb G E 2000a Measured and modeled properties of mammalian skeletal muscle: III. The effects of stimulus frequency on stretch-induced force enhancement and shortening-induced force depression *J. Muscle Res. Cell Motil.* **21** 21–31

Brown I E and Loeb G E 2000b Measured and modeled properties of mammalian skeletal muscle IV Dynamics of activation and deactivation *J. Muscle Res. Cell Motil.* **21** 33–47

Chan S S and Moran D W 2006 Computational model of a primate arm from hand position to joint angles joint torques and muscle forces *J. Neural Eng.* **3** 327–37

Cheng E J, Brown I E and Loeb G E 2000 Virtual muscle a computational approach to understanding the effects of muscle properties on motor control *J. Neurosci. Methods* **101** 117–30

Hamilton A F D and Wolpert D M 2002 Controlling the statistics of action Obstacle avoidance *J. Neurophysiol.* **87** 2434–40

Harris C M and Wolpert D M 1998 Signal-dependent noise determines motor planning *Nature* **394** 780–84

Jones K E, Hamilton A F D and Wolpert D M 2002 Sources of signal-dependent noise during isometric force production *J. Neurophysiol.* **88** 1533–44

Lan N, Li Y, Sun Y and Yang F S 2005 Reflex regulation of antagonist muscles for control of joint equilibrium position *IEEE Trans. Neural Syst. Rehabil. Eng.* **13** 60–71

Mileusnic M P and Loeb G E 2006 Mathematical models of proprioceptors: II. Structure and function of the Golgi tendon organ *J. Neurophysiol.* **96** 1789–1802

Scott S H and Loeb G E 1995 Mechanical properties of aponeurosis and tendon of the cat soleus muscle during whole-muscle isometric contractions *J. Morphol.* **224** 73–86

Selen L P J, Beek P J and van Dieen J H 2005 Can co-activation reduce kinematic variability a simulation study *Biol. Cybern.* **93** 373–81

Singh K, Richmond F J R and Loeb G E 2000 Recruitment properties of intramuscular and nerve-trunk stimulating electrodes *IEEE Trans. Rehabil. Eng.* **8** 276–85

Song D, Lan N, Loeb G E and Gordon J Model-based sensorimotor integration for multi-joint control—development of a virtual arm model *Annu. Biomed. Eng.* at press doi: 10.1007/s10439-008-9461-8

Song D, Raphael G, Lan N and Loeb G E 2007 *Improvement in Computational Efficiency of Virtual Muscle Model* (Los Angeles: BMES)

Zajac F E 1989 Muscle and tendon—properties, models, scaling, and application to biomechanics And motor control *Crit. Rev. Biomed. Eng.* **17** 359–411